Structural Basis for Phosphomannose Isomerase Activity in Phosphoglucose Isomerase from *Pyrobaculum aerophilum*: A Subtle Difference between Distantly Related Enzymes†

Michael K. Swan,‡ Thomas Hansen,§ Peter Schönheit,§ and Christopher Davies*,‡

Department of Biochemistry and Molecular Biology, Medical University of South Carolina, Charleston, South Carolina 29425, and Institut für Allgemeine Mikrobiologie, Christian-Albrechts-Universität Kiel, D-24118 Kiel, Germany

Received July 1, 2004; Revised Manuscript Received August 23, 2004

ABSTRACT: The crystal structure of a dual-specificity phosphoglucose/phosphomannose isomerase from the crenarchaeon *Pyrobaculum aerophilum* (PaPGI/PMI) has been determined in complex with glucose 6-phosphate at 1.16 Å resolution and with fructose 6-phosphate at 1.5 Å resolution. Subsequent modeling of mannose 6-phosphate (M6P) into the active site of the enzyme shows that the PMI activity of this enzyme may be due to the additional space imparted by a threonine. In PGIs from bacterial and eukaryotic sources, which cannot use M6P as a substrate, the equivalent residue is a glutamine. The increased space may permit rotation of the C2−C3 bond in M6P to facilitate abstraction of a proton from C2 by Glu203 and, after a further C2−C3 rotation of the resulting *cis*-enediolate, re-donation of a proton to C1 by the same residue. A proline residue (in place of a glycine in PGI) may also promote PMI activity by positioning the C1−O1 region of M6P. Thus, the PMI reaction in PaPGI/PMI probably uses a *cis*-enediol mechanism of catalysis, and this activity appears to arise from a subtle difference in the architecture of the enzyme, compared to bacterial and eukaryotic PGIs.

Phosphoglucose isomerase (PGI,[1] EC 5.3.1.9) and phosphomannose isomerase (PMI, EC 5.3.1.8) are aldose-ketose isomerases that catalyze the reversible interconversion of glucose 6-phosphate (G6P) to fructose 6-phosphate (F6P) and mannose 6-phosphate (M6P) to F6P, respectively. Several aerobic crenarcheaons, including *Aeropyrum pernix*, *Thermoplasma acidophilum*, and *Pyrobaculum aerophilum*, contain a dual-specificity PGI/PMI, which catalyzes PGI and PMI activities at equal rates (*1*, *2*). Since both isomerizations are equilibrium reactions, this enzyme can also interconvert glucose 6-phosphate and mannose 6-phosphate and hence is also a C2 epimerase. These enzymes have very low levels of sequence identity with "conventional" PGIs from eukarya and bacteria and so constitute a distinct phylogenetic group within the PGI superfamily (*1*). No recognizable *pmi* gene can be identified within the genomes of these archaea, so *in vivo*, this enzyme may fulfill the biological roles of both a PGI and a PMI. Although only remotely related (*1*, *3*), the protein from *P. aerophilum* is structurally similar to conventional PGI enzymes (*4*). At the active site level, in particular, this structure is surprisingly well conserved with bacterial and eukaryotic PGIs and supports a common mechanism for the phospho*glucose* isomerase reaction throughout the PGI superfamily (*4*). This comprises proton transfer between C2 (of G6P) and C1 (of F6P) catalyzed by a glutamate base, and it proceeds via a *cis*-enediol(ate) intermediate (*5*−*7*). The mechanism of the PMI reaction, however, is interesting because conventional PGI enzymes are highly specific for their substrates, glucose 6-phosphate (G6P) and fructose 6-phosphate (F6P) (see ref *8*), and will not isomerize mannose 6-phosphate to F6P except at an extremely low rate (*9*). How PMI activity can occur within a PGI is something of a quandary because a proton must be transferred across different faces of the bound substrates: the *re-re* face of G6P and the *si-si* face of M6P. Two possible mechanisms have been proposed by Seeholzer to explain PMI activity in a PGI (*9*). One is to use a second base catalyst in the active site that can abstract protons from the *si-si* face of the substrate; the reaction, therefore, proceeds via a *trans*-enediol intermediate. The other is to rotate the C2−C3 substrate bond of the enediolate intermediate, i.e., after abstraction of a proton from C2 and prior to donation of a proton to C1 (in the G6P to F6P direction). The lack of a second base catalyst in the active site of PGI/PMI from *P. aerophilum* (*4*) shows that the former hypothesis is unlikely, but, for the second hypothesis, it is unclear how a C2−C3 rotation can be accommodated within the architecture of an active site that is highly similar to those PGIs that cannot isomerize M6P.

We have determined the structures of PGI/PMI from *P. aerophilum* in complex with G6P at 1.16 Å resolution and with F6P at 1.5 Å resolution. Using these structures,

† This work was supported in part by a grant from the Deutsche Forschungsgemeinschaft to P.S. (SCHO 316/9-1).

* To whom correspondence should be addressed: Department of Biochemistry and Molecular Biology, Medical University of South Carolina, 173 Ashley Ave., Charleston, SC 29425. Telephone: (843) 792-1468. Fax: (843) 792-8568. E-mail: davies@musc.edu.

‡ Medical University of South Carolina.

§ Christian-Albrechts-Universität Kiel.

[1] Abbreviations: F6P, fructose 6-phosphate; G6P, glucose 6-phosphate; PGI, phosphoglucose isomerase; PaPGI/PMI, phosphoglucose isomerase/phosphomannose isomerase from *P. aerophilum*; M6P, mannose 6-phosphate.

10.1021/bi048608y CCC: $27.50 © 2004 American Chemical Society
Published on Web 10/12/2004

mannose 6-phosphate was modeled into the active site, and this revealed that PMI activity may result from an approximately 60° rotation of the substrate about its C2−C3 bond. This rotation appears to be permitted by the presence of a threonine in PGI/PMI, whereas in conventional PGIs, it is prevented by a glutamine. Hence, a surprisingly subtle alteration in the active site architecture could be responsible for the lowered specificity of a normally highly specific enzyme.

EXPERIMENTAL PROCEDURES

The crystallization of PGI/PMI from *P. aerophilum* (PaPGI/PMI) has been described previously (*3*). These crystals belong to space group $P2_1$ with the following cell dimensions: $a = 55.1$ Å, $b = 100.8$ Å, $c = 55.8$ Å, and $\beta = 113.2°$. The crystals were cryoprotected over a period of several hours by being passed through a series of mother liquor solutions [25% polyethylene glycol 8000 (w/v) and 0.22 M ammonium sulfate, buffered with 0.1 M Tris-HCl (pH 8.5)] containing increasing concentrations of glycerol up to a maximum of 26%. Crystals were then soaked in the same solution but also with one of the three substrates: glucose 6-phosphate (G6P), fructose 6-phosphate (F6P), and mannose 6-phosphate (M6P). Substrate concentrations used for these experiments ranged between 5 and 20 mM with soak times ranging from 1 to 24 h, and in all cases, crystals were incubated at 21 °C.

Data were collected on a MAR225 CCD detector (MAR-USA) at SER-CAT beamline ID22 at the Advanced Photon Source (APS, Argonne National Laboratory, Argonne, IL). The data collection parameters were as follows: a crystal-to-detector distance of 100 mm, an oscillation angle of 0.5°, an exposure time of 1 s per image, and 360° of data acquired. The data were processed using the HKL2000 software package (*10*). Substrate molecules were identified by refinement of the native model (*4*) against the substrate-soaked data, followed by examination of the $|F_o| - |F_c|$ difference electron density map. After the ligand molecule had been fitted, the respective structures were refined using REFMAC5 (*11*) and manual improvements were made with XTALVIEW (*12*). Solvent atoms were introduced using ARP/wARP (*13*). Side chains with multiple conformations and anisotropic temperature factors were also refined. To visualize how a molecule of M6P would fit into the active site, the PaPGI/PMI−G6P complex was used as a template to model M6P, using XTALVIEW. Coordinates and structure factors have been submitted to the Protein Data Bank (entry 1X9I for the complex with G6P and 1X9H for the complex with F6P).

RESULTS

Crystal Structure Determination. The structure of PaPGI/PMI has been determined previously (*4*) and will be described only briefly. The structure is a dimer of identical subunits. Each subunit contains two domains, both built around parallel β-sheets. Although there is no detectable sequence similarity, except in two of the six active site motifs, the structure resembles the core of a classic PGI-like fold and so does belong to the PGI superfamily.

All three soaking experiments generated strong $|F_o| - |F_c|$ density within both active sites of the dimer. In high-resolution structures, these substrates can be discerned easily; G6P and M6P are epimers at C2, and F6P can be distinguished from G6P by trigonal planar geometry at C2, due to the keto group, in contrast to the tetrahedral geometry at C2 of G6P or M6P. Interestingly, a soak in G6P generated F6P, a soak in M6P generated G6P, and soaking in F6P produced F6P and thus demonstrated the activity of the enzyme within the crystal at 21 °C, a temperature far removed from the optimum for PaPGI/PMI activity of ∼100 °C (*2*). This activity adds credence to the validity of these structures as representative of the enzyme *in vivo*.

Table 1: Data Collection and Refinement Statistics of the Structures in Complex with Fructose 6-Phosphate (F6P) and Glucose 6-Phosphate (G6P)[a]

	F6P	G6P
Data Collection		
soak molarity (mM)	5	5
soak time (h)	6	12
resolution of data (Å)	36.0−1.50 (1.55−1.50)	36.0−1.16 (1.20−1.16)
no. of measured reflections	310815	1244188
no. of unique reflections	86757	176109
completeness (%)	96.8 (82.8)	90.0 (77.5)
mean $I > \sigma I$	19.5 (1.7)	40.4 (4.0)
R_{merge}[b]	6.3 (39.1)	4.9 (23.3)
Refinement		
resolution range (Å)	36.0−1.50	36.0−1.16
no. of water molecules	403	559
R factor (%)	15.3	14.8
R_{work} (%)	15.2	14.7
R_{free} (%)	18.0	16.4
rms deviations from ideal stereochemistry		
bond lengths (Å)	0.010	0.007
bond angles (deg)	1.34	1.33
B factors		
mean *B* factor (main chain) (Å^3)	16.5	12.1
rms deviation in main chain *B* factor (Å^3)	0.41	0.43
mean B factor (side chains and waters) (Å^3)	20.5	16.0
rms deviation in side chain *B* factors (Å^3)	1.16	1.02
Ramachandran plot		
% residues in most favored region	93.9	95.0
% residues in additionally allowed regions	5.7	4.8
% residues in generously allowed regions	0.4	0.2
% residues in disallowed regions	0.0	0.0

[a] Numbers in parentheses are for the outer shell of data. [b] Where $R_{merge} = \sum_{hkl}\sum_i|I_i(hkl) - \langle I(hkl)\rangle|/[\sum_{hkl}\sum_i I_i(hkl)]$.

The complex with G6P was determined at 1.16 Å resolution and the structure refined to an *R*-factor of 14.8% ($R_{free} = 16.4\%$) (Table 1). The resulting $|F_o| - |F_c|$ density in the active site was modeled as G6P due to the configuration and geometry at C2 (Figure 1). The contacts between the enzyme and the substrate are shown in Figure 1b. Most of the contacts are clustered at each end of the substrate, i.e., around the phosphate and around the C1−C2 region. The sugar phosphate is held by potential hydrogen bonds with Ser48, Ser87, Ser89, Thr92, and a single water molecule. The O5 hydroxyl is within hydrogen bonding distance of both Lys298 and His219 (the latter from the partner subunit of the dimer). O4 forms only one hydrogen bond with the amide nitrogen of Gly47, as does O3 with the carbonyl group of His219.

In the isomerization reaction catalyzed by PGI, the site of proton transfer is between C1 and C2. In the PaPGI/PMI−

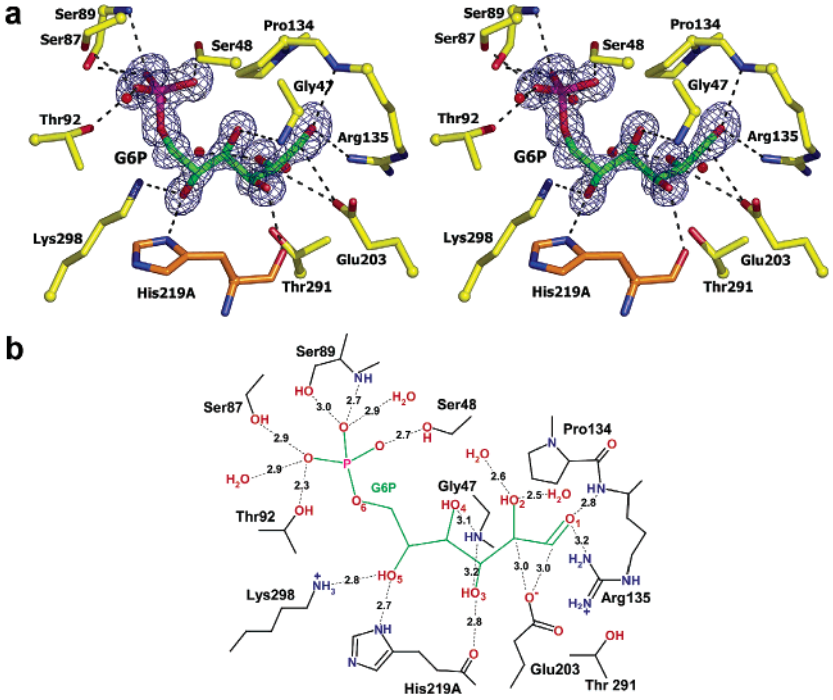

FIGURE 1: Structure of PGI/PMI from *P. aerophilum* in complex with glucose 6-phosphate (G6P), at 1.16 Å resolution. (a) Stereoview showing G6P bound to the active site region. Shown is the active site from subunit B, but the contacts are essentially identical in subunit A. The electron density shown around the substrate in blue is an unbiased ($|F_o| - |F_c|$) difference map, calculated from the final coordinates refined in the absence of ligand. The side chains of those residues surrounding the ligand are shown in a bond form in which carbon, oxygen, and nitrogen are colored yellow, red, and blue, respectively, except for His219 which is colored orange to indicate it is part of subunit A. G6P is colored with green bonds. Water molecules are shown as red spheres. Important contacts are shown as dashed lines. The figure was produced using PYMOL (*25*). (b) Diagram of the distances (in angstroms) between atoms of G6P (colored green) and of amino acids in the active site (colored black).

G6P structure, the hydroxyl group at C2 of G6P forms no direct contacts with the protein but is close to two water molecules. The C1 carbonyl contacts both the amide nitrogen and side chain guanidinium group of Arg135. Exactly the same arrangement is seen in a crystal structure of mouse PGI in complex with G6P (*14*), in which the residue equivalent to Arg135 is Arg272. The Oϵ1 carboxylate atom of Glu203, the putative base catalyst, is equidistant (3.0 Å) from the carbons at positions 1 and 2. The overall similarity in substrate binding modes between PaPGI/PMI and conventional PGIs is evidence that the mechanism of phospho*glucose* isomerase activity in the two enzymes is the same.

Soaking in G6P or F6P produced a structure of PaPGI/PMI in complex with F6P, and these structures are experimentally identical. However, the structure produced by soaking in G6P was determined at a higher resolution (1.5 Å) and so is presented here. This was refined to an *R*-factor of 15.3% (R_{free} = 18.0%), and examination of the $|F_o| - |F_c|$ density in both active sites showed clearly the trigonal planar geometry at C2 that defines this ligand as F6P (Figure 2a). The enzyme−substrate contacts are essentially the same as in the complex with G6P with only very minor differences in the contact distances in the C1−C2 region, to Glu203 and Arg135 (Figure 2b). This exemplifies the similarity of these substrates when bound in straight-chain form. The main difference is the presence of only one water molecule near O2 of F6P rather than the two seen near this atom in the G6P-bound complex.

Conformational Changes upon Ligand Binding. Characteristic of PGIs from bacterial and eukaryotic sources are conformational changes in the protein that occur due to the binding of inhibitor or substrate molecules. These shifts result in the closure of active site loops around the ligand and are probably important for catalysis (*7*, *15*, *16*). To determine whether similar conformational changes are required in PaPGI/PMI, the two substrate-bound structures were compared with the native structure. Both structures superimposed very closely with the native structure with rms deviations between all main chain atoms of 0.16 Å for the G6P structure and 0.23 Å for F6P. Almost no structural differences were apparent between the native and substrate-bound structures, including all residues that comprise the active site (not shown). The same was seen when the native structure was compared to an inhibitor-bound structure of PaPGI/PMI (*4*). Hence, conformational changes in PaPGI/PMI do not appear to be required for catalytic activity, and this may be a consequence of the constraints on the protein architecture due to the extreme thermostability of the enzyme.

Modeling of Mannose 6-Phosphate. An unfortunate consequence of the activity of PaPGI/PMI in crystalline form was our inability to generate an experimental complex with M6P. To gain insight into the mechanism of this enzyme as a phospho*mannose* isomerase, we modeled a molecule of M6P into the active site of the enzyme using the G6P-bound structure as a template. G6P and M6P are C2 epimers and so differ only in the configuration at C2. Hence, M6P can be positioned to superimpose with G6P except for the hydroxyl at C2. For G6P, this group occupies the space between Pro134 and Arg135, whereas in M6P, it makes a close contact with Glu203 (approximately 2.2 Å), showing that this binding mode for M6P is unlikely. Moreover, in this position for M6P, in which the proton at C2 would point

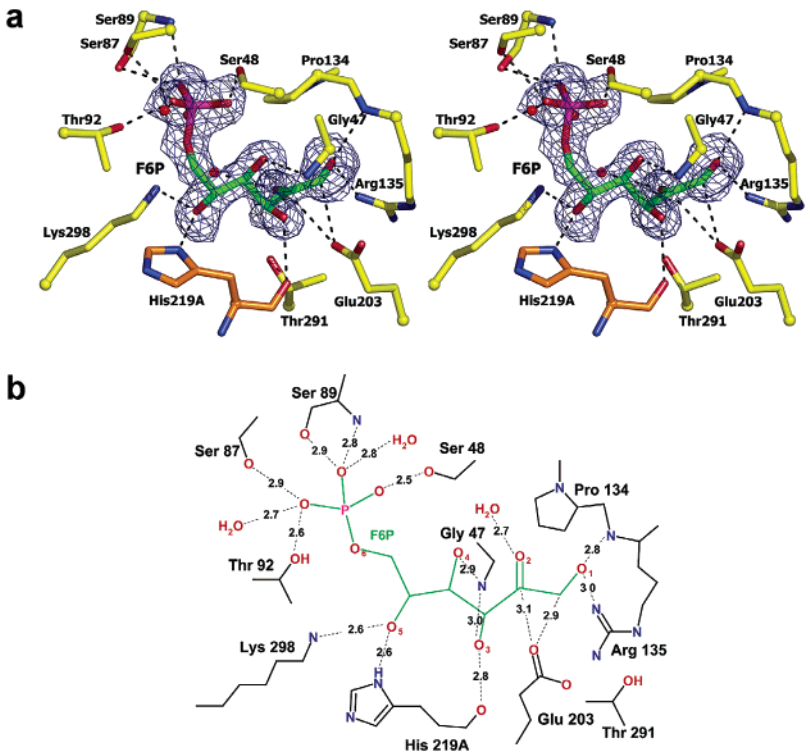

FIGURE 2: Structure of PGI/PMI from *P. aerophilum* in complex with fructose 6-phosphate (F6P), at 1.5 Å resolution. (a) Stereoview showing F6P bound to the active site region of PaPGI/PMI. The electron density and the coloring scheme are the same as described for Figure 1. As in Figure 1, subunit B of the dimer is shown but the contacts are virtually identical in subunit A. (b) Diagram of the distances (in angstroms) between atoms of F6P (colored green) and of amino acids in the active site (colored black).

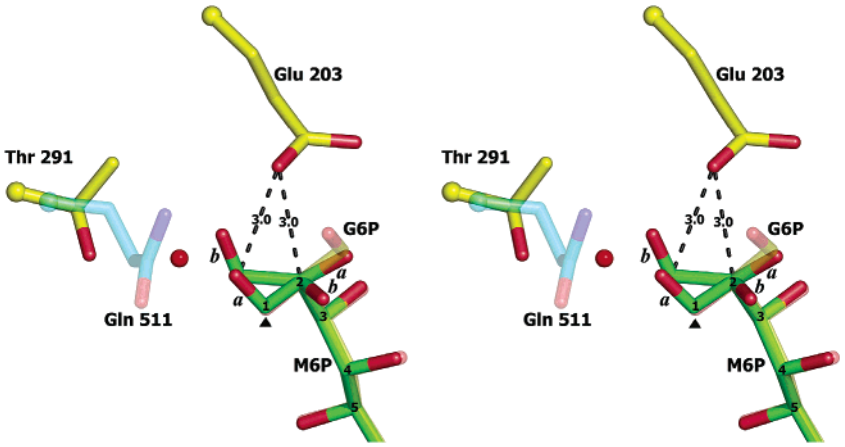

FIGURE 3: Structural basis for phosphomannose isomerase activity of PGI/PMI from *P. aerophilum*. This stereoview shows a close-up of the active region where isomerization takes place. A model of M6P (colored as green bonds) was modeled into the active site of PaPGI/PMI by superimposing it onto G6P (colored as yellow bonds), using the G6P-bound structure as a template, and is shown in two positions. In position *a*, the substrate is well placed for abstraction of a proton by Glu-203 from C2. A rotation of approximately 60° about the C2−C3 bond of M6P generates position *b*, in which C1 is now sufficiently close for re-donation of the proton back from the glutamate. Such a rotation would appear to be blocked in conventional PGIs [represented here by rabbit PGI (*16*)] by the presence of Gln511 (shown as blue bonds), whereas it is permitted in PaPGI/PMI because this space is occupied by a water molecule (red sphere) and Thr291. The position of O2 in G6P is denoted with the black triangle. This figure was produced using PYMOL (*25*).

away from Glu203 and toward Pro134, there are no suitable residues in this region of the active site that could abstract the C2 proton. A more favorable binding orientation can be modeled by rotation of the C2−C3 bond to move the C2 hydroxyl of M6P away from Glu203 such that it occupies the same position as C1 of G6P. Compared to that of G6P, this binding mode of M6P is "reversed"; i.e., its C2−O2 bond overlaps with the C1−C2 bond of G6P, and its C1−C2 bond overlaps with the C2−O2 bond of G6P. The C1−O1 bond lies between Arg135 and Pro134, and O1 points toward a water molecule (present in the G6P-bound structure), which, in turn, is hydrogen-bonded to Thr291 (Figure 3). Such a water molecule could easily be displaced during the binding of M6P. An alternative mechanism for binding is that a slight movement of Glu203 could help accommodate the C2 hydroxyl of M6P, but this is considered unlikely due to the critical importance of this residue for proton abstraction.

The result of the modeling is a position for M6P in which C2 is placed perfectly for its proton to be abstracted by Glu203 from its *si* face. At this point, though, a problem arises because the recipient of this proton, C1, is located on

the opposite side, compared to its counterpart in G6P, and well beyond the reach of Glu203. M6P must, therefore, undergo a rearrangement to bring this atom closer to Glu203. A rotation of approximately 60° is sufficient to bring C1 to within 3 Å of Glu203 (the same as the distance between C1 and C2 in the G6P-bound structure) (Figure 3). This rotation appears to be permitted because of the space between Glu203, Arg135, and Thr291 but probably occurs in only one direction (clockwise as viewed from C2 to C3); otherwise, the C2 oxygen would again be too close to Glu203. It is interesting to note that, in conventional PGIs, Thr291 is replaced with a glutamine [see, for example, rabbit PGI (*16*)]. Thus, there appears to be more room within the active site of PaPGI/PMI to accommodate the C1 group of M6P, compared to conventional PGIs. In addition, the substitution of a glycine (Gly271 in rabbit PGI) with a proline (Pro134 in PaPGI/PMI) may also contribute to PMI activity by positioning the C1−O1 group of M6P. Thus, when compared to activities of conventional PGIs, PMI activity in PaPGI/PMI may arise from just two amino acid differences and can be visualized without invoking any conformational changes in the protein and with only minor adjustments to the substrate.

DISCUSSION

The high degree of conservation between the active site residues of PaPGI/PMI and those of PGIs from bacterial and eukaryotic sources confirms this protein as a member of the PGI superfamily (*4*). Its mechanism of phosphoglucose isomerase activity, therefore, is conserved throughout the PGI superfamily. Key to this isomerization is Glu203, which abstracts a proton from C2 of G6P and donates it to C1 to form F6P (or vice versa in the reverse direction). The intermediate in the reaction is a *cis*-enediolate. The amino acids that catalyze ring opening are also conserved in PaPGI/PMI. These are His219, which donates a proton to the ring oxygen, and Lys298, which appears to assist this process by concomitantly abstracting a proton from C1 of G6P (or C2 of F6P) (*14*). The presence of these latter residues in PaPGI/PMI shows that, even at the very high temperature at which *P. aerophilum* exists (*17*), catalyzed ring opening of sugars is required for metabolism.

Although the mechanism of phospho*glucose* isomerization is clear, the interest in this enzyme stems from its dual activity as a phospho*mannose* isomerase because the specificity of conventional PGI (e.g., rabbit PGI) is essentially absolute for G6P and F6P (*8*), and PMI activity cannot be detected except at very low and nonphysiological rates (*9*).

How a PGI Catalyzes PMI Activity. At first sight, it would not appear to be difficult for a PGI to catalyze PMI activity; both reactions are aldose-ketose isomerizations, and both involve the transfer of a proton between C1 and C2 (aldose to ketose direction). But in fact, the reversal of the configuration at C2 between G6P and M6P creates a mechanistic challenge because the proton must be removed from the opposite side of the substrate in M6P, compared to G6P (*5*). This means that for a PGI to interconvert M6P to F6P, a single base cannot easily abstract and re-donate a proton with the same ease as in the G6P to F6P conversion. One solution to this problem is for the active site to contain a second base (see ref *9*) so that protons can be abstracted and/or donated on both faces of the substrate. However, this is ruled out in PaPGI/PMI by the lack of any other residues in the active site with the potential to act as a base within reach of the C1−C2 region of the substrates. Clearly then, another mechanism must operate for the PMI activity of PaPGI/PMI. An alternative is the rotation of the C2−C3 substrate bond after proton abstraction and before proton re-donation (*9*), and this would permit the same base to be used for both abstractions on both faces. Presumably, conventional PGIs achieve their high specificity for G6P over M6P (for isomerization) by preventing such a rotation, and it has been argued that a glutamine serves this purpose (Gln511 in rabbit PGI) by blocking rotation of the C1−O1 group (*14*). In PaPGI/PMI, however, the residue equivalent to Gln511 is Thr291, and the smaller size of this residue leaves more room within this critical region of the active site. Related PGI/PMIs from other crenarcheaons, such as *A. pernix* and *T. acidophilum*, contain either a threonine, a leucine, or a valine in this position (*1*).

With a threonine in place of a glutamine at position 291, the binding of M6P within the active site of PaPGI/PMI can now be envisaged relatively easily because there is sufficient space in front of Thr291 to accommodate the C1−O1 group of M6P (see Figure 3). Moreover, its C2 is now optimally placed for its proton to be abstracted by Glu203 from the *si* face; however, a 60° rotation about the C2−C3 bond is then required to bring C1 within 3 Å of Glu203 (see Figure 3) for proton re-donation at the *re* face of the *cis*-enediolate. Again, this C2−C3 rotation appears to be permitted due to the increased space in the active site imparted by Thr291. Pro134 may also promote PMI activity by helping to position the C1−O1 group of M6P. In conventional PGI, this residue is a glycine (i.e., Gly271 in rPGI). Hence, the altered amino acids, Gln to Thr and Gly to Pro, together may constitute the subtle difference between a PGI that is specific for G6P and one with a broader specificity that can also utilize M6P (a PMI). By extension, because both reactions are reversible, it also defines PaPGI/PMI as a C2 epimerase.

The C2−C3 rotation, postulated to occur in PaPGI/PMI during the interconversion of M6P and F6P, does not appear to have any negative impact on the catalytic efficiency of the enzyme as a PMI compared to its PGI activity, suggesting there is little or no barrier to this rotation of the substrate within the active site of the enzyme. In fact, the catalytic efficiency (V_{max}/K_m) of the enzyme is actually higher for M6P than for G6P (234 and 79 units mg^{-1} mM^{-1}, respectively) (*2*). This is partly due to the lower K_m that PaPGI/PMI has for M6P compared to G6P, and one can speculate that, by positioning the C1−O1 group, Pro134 may contribute to the higher affinity for M6P.

The catalytic mechanism of conventional PMI enzymes has yet to be established (see, for example, ref *18*), but it is likely to be distinct from that catalyzed by PaPGI/PMI. A key difference is that all known PMIs are metalloenzymes and typically contain a Zn^{2+} that is required for catalysis (*19*). Furthermore, PMIs do not manifest anomerase or epimerase activities (*9*, *20*), suggesting that rotations of substrate bonds are prevented within the active site of these enzymes, possibly by the coordination of the C1 hydroxyl and C2 carbonyl by the zinc ion (*21*). By contrast, rotation about the C2−C3 bond is a critical aspect of the PMI mechanism in PaPGI/PMI.

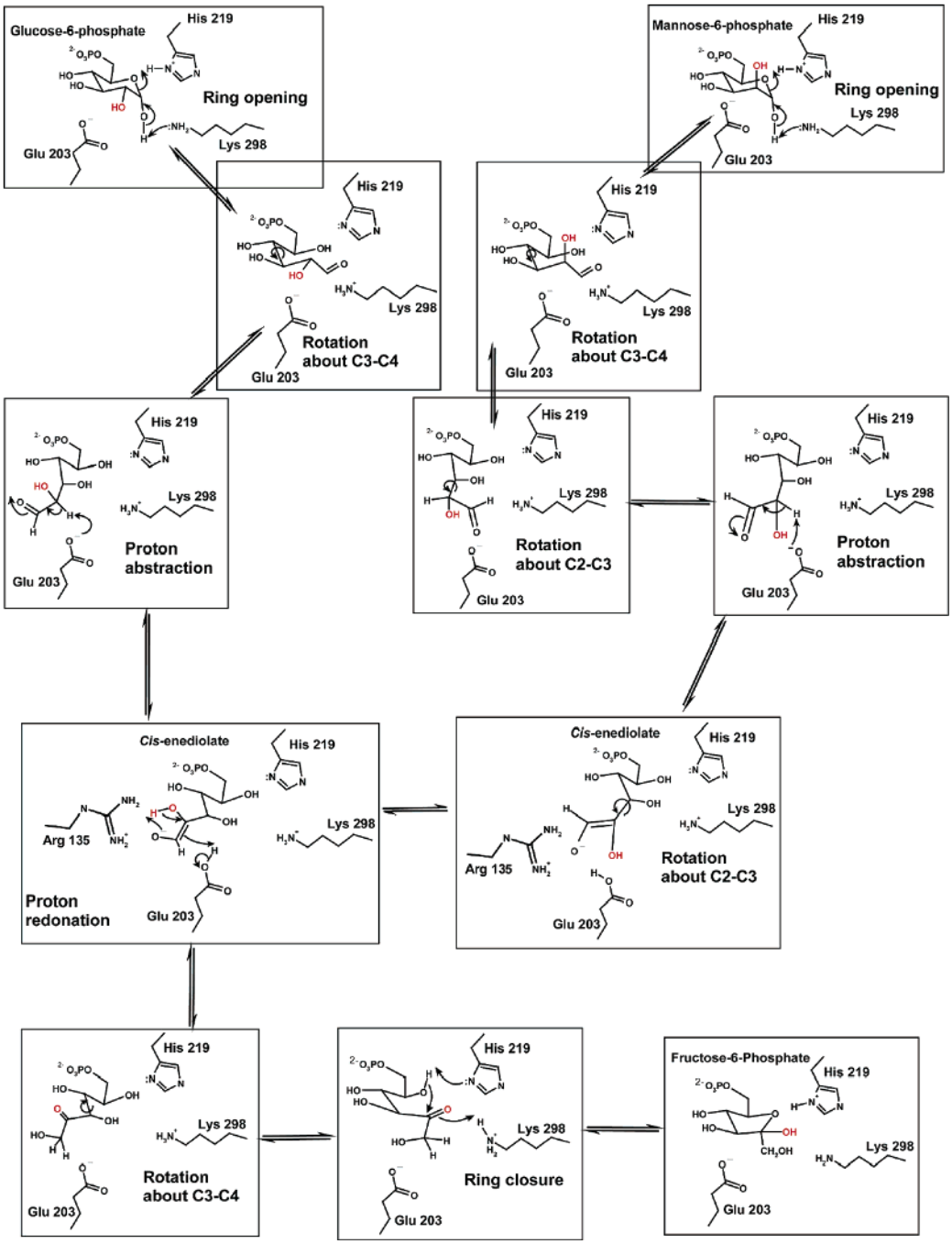

FIGURE 4: Mechanism of phosphoglucose and phosphomannose isomerizations catalyzed by PGI/PMI from *P. aerophilum*. The two aldose substrates, G6P and M6P, are shown at the top, and the F6P product is at the bottom right. Each substrate undergoes ring opening, a C3−C4 rotation to position the C1−C2 region near Glu203, and a proton abstraction to form a *cis*-enediolate intermediate. Then, the same steps in reverse lead to the formation of the product. For M6P to be isomerized into F6P or epimerized into G6P, two additional rotations of the substrate, both around the C2−C3 axis, are required. One rotation positions C2 for abstraction of a proton by Glu-203, and the other rotates the *cis*-enediolate prior to proton re-donation at C1, also by Glu203. The oxygen at C2 that differs in configuration between G6P and M6P is shown in red.

A C3−C4 Rotation Is Required after Ring Opening. At first sight, the C2−C3 rotation of its substrate is not unique for a PGI because such a rotation occurs in conventional PGI during the anomerization of F6P [see Seeholzer (*9*)] and likely also in PaPGI/PMI. How then do conventional PGIs permit a C2−C3 rotation of F6P without generating PMI activity as a byproduct? The answer comes from the locations of these respective rotations. Two C2−C3 rotations are predicted in the PMI mechanism, and since one of these occurs between proton abstraction and proton re-donation, it must take place at the site of isomerization. However, for the C2−C3 rotation used to anomerize F6P, there is no such stipulation and the rotation can occur directly after ring opening while the substrate remains in the ring shape. Model building experiments in both mouse PGI and PaPGI/PMI show sufficient room for such rotations when substrates remain in the ring shape (not shown). Thus, to maintain high specificity for G6P over M6P in the isomerization reaction catalyzed by conventional PGI, a C2−C3 rotation is permitted in one region of the active site but not in another, i.e., near the base catalyst glutamate. A fundamental consequence of this separation is the requirement for a rearrangement of

the substrate after ring opening for the transport of the C1−C2 region of the substrate to a position near the glutamate base catalyst. A crystal structure of mouse PGI in complex with G6P, in both ring and straight chain forms (*14*), shows that this can most easily be achieved by an ∼180° rotation of the C3−C4 bond. The same conclusion was drawn from an earlier structural comparison of rabbit PGI bound by ring form F6P and the same enzyme in complex with the inhibitor, 5-phosphoarabinonate (PAB) (*22*). This resolves the long-standing issue of why inhibitors of PGI mimic straight chain sugars [e.g., PAB (*23*)] even though the apparent substrate for the enzyme exists predominantly in the ring form (*24*).

Overall Mechanism for PGI and PMI Activities. The high-resolution structural data of PaPGI/PMI presented here can be summarized in a comprehensive reaction scheme encompassing the PGI, PMI, and epimerase activities of this enzyme, shown in Figure 4. In the first step, one of the three substrates (G6P, F6P, or M6P) binds in ring form and ring opening is catalyzed by His219, acting as an acid catalyst by donating a proton to O5, and Lys298, acting as a base catalyst and abstracting a proton from O1 of G6P and M6P or O2 of F6P. A role for Lys518 in rabbit PGI (the equivalent of Lys298 in PaPGI/PMI) in ring opening has been postulated previously in two different mechanisms. In one mechanism, Lys518 (acting as an acid) was proposed to protonate the ring oxygen (*6*), and in another (acting as a base), it helps abstract a proton from O2 of F6P via a bridging water molecule (*22*). By contrast, in the current mechanism, Lys298 is sufficiently close to act directly as a base on O2 of F6P and O1 of G6P without any requirement for a water molecule.

After ring opening, the C1−C2 region is too far away from Glu203, the base catalyst for both of the isomerization reactions. A rearrangement of the three substrates, primarily through an ∼180° rotation of the C3−C4 bond, swings their respective C1−C2 regions close to Glu203. After this, G6P and F6P are appropriately positioned for proton abstraction from C2 and C1, respectively, but for M6P, an additional rotation about the C2−C3 bond is required to orient its C2 proton toward Glu203. In all cases, the intermediate formed after proton abstraction is a *cis*-enediolate, which for G6P and F6P is stabilized by Arg135. For the formation of F6P from G6P and vice versa, re-donation of the proton to C1 (or C2) is straightforward because the carboxylate oxygen is equidistant from both C1 and C2 and because proton abstraction and donation both take place on the *re-re* face of the substrate. In the case of M6P, however, the *cis*-enediolate intermediate must first rotate 60° about the C2−C3 bond (as described above) before proton re-donation at C1 is possible. This rotation is in essence an epimerization because M6P now joins the G6P/F6P branch of the reaction scheme and from this point can form G6P as well as F6P (as illustrated by the conversion of M6P to G6P in the crystal soaking experiments). To complete the reaction, a C3−C4 rotation restores the ring shape of the respective substrates, followed by ring closure using the His219/Lys298 system acting in reverse.

The mechanisms for PGI and PMI activities in PaPGI/PMI, then, appear to be very similar, and despite the mechanistic challenge of the different configuration at C2 for the two aldose substrates, a slightly more open active site created in part by the presence of a threonine in place of a glutamine in conventional PGIs may be responsible for the dual activity as a PGI and a PMI rather than as a strict PGI. The same situation may also apply to other PGI/PMIs, which contain leucine or valine at the same position (*1*). Of course, this hypothesis must now be tested by site-directed mutagenesis experiments, beginning with Thr291 and then extending to include other residues such as Pro134 that may also contribute to PMI activity.

ACKNOWLEDGMENT

Data were collected at Southeast Regional Collaborative Access Team (SER-CAT) beamline 22-ID at the Advanced Photon Source. Supporting institutions may be found at www.ser-cat.org/members.html. Use of the Advanced Photon Source was supported by the U.S. Department of Energy, Office of Science, Office of Basic Energy Sciences, under Contract W-31-109-Eng-38. We acknowledge the assistance of Zhongmin Jin in the collection of the F6P data set used in this study. We also thank Graham Solomons for his critical reading of the manuscript.

REFERENCES

1. Hansen, T., Wendorff, D., and Schönheit, P. (2004) Bifunctional phosphoglucose/phosphomannose isomerases from the Archaea *Aeropyrum pernix* and *Thermoplasma acidophilum* constitute a novel enzyme family within the phosphoglucose isomerase superfamily, *J. Biol. Chem. 279*, 2262−2272.
2. Hansen, T., Urbanke, C., and Schönheit, P. (2004) Bifunctional phosphoglucose/phosphomannose isomerase from the hyperthermophilic archaeon *Pyrobaculum aerophilum*, *Extremophiles* (in press).
3. Swan, M. K., Hansen, T., Schönheit, P., and Davies, C. (2004) Crystallisation and preliminary X-ray diffraction analysis of phosphoglucose/phosphomannose isomerase from *Pyrobaculum aerophilum*, *Acta Crystallogr. D60*, 1481−1483.
4. Swan, M. K., Hansen, T., Schönheit, P., and Davies, C. (2004) A novel phosphoglucose isomerase/phosphomannose isomerase from the crenarchaeon *Pyrobaculum aerophilum* is a member of the PGI superfamily: structural evidence at 1.16 Å resolution, *J. Biol. Chem. 279*, 39838−39845.
5. Rose, I. A. (1975) Mechanism of the aldose-ketose isomerase reactions, *Adv. Enzymol. Relat. Areas Mol. Biol. 43*, 491−517.
6. Jeffery, C. J., Hardre, R., and Salmon, L. (2001) Crystal structure of rabbit phosphoglucose isomerase complexed with 5-phospho-D-arabinonate identifies the role of Glu357 in catalysis, *Biochemistry 40*, 1560−1566.
7. Read, J., Pearce, J., Li, X., Muirhead, H., Chirgwin, J., and Davies, C. (2001) The crystal structure of human phosphoglucose isomerase at 1.6 Å resolution: implications for catalytic mechanism, cytokine activity and haemolytic anaemia, *J. Mol. Biol. 309*, 447−464.
8. Noltmann, E. A. (1972) in *The Enzymes* (Boyer, P. D., Ed.) pp 271−354, Academic Press, New York.
9. Seeholzer, S. H. (1993) Phosphoglucose isomerase: a ketol isomerase with aldol C2-epimerase activity, *Proc. Natl. Acad. Sci. U.S.A. 90*, 1237−1241.
10. Otwinowski, Z., and Minor, W. (1997) Processing of X-ray diffraction data collected in oscillation mode, *Methods Enzymol. 276*, 307−326.
11. Murshudov, G. N., Vagin, A. A., and Dodson, E. J. (1997) Refinement of macromolecular structures by the maximum-likelihood method, *Acta Crystallogr. D53*, 240−255.
12. McRee, D. E. (1999) XtalView/Xfit: A versatile program for manipulating atomic coordinates and electron density, *J. Struct. Biol. 125*, 156−165.
13. Perrakis, A., Harkiolaki, M., Wilson, K. S., and Lamzin, V. S. (2001) ARP/wARP and molecular replacement, *Acta Crystallogr. D57*, 1445−1450.
14. Solomons, J. T., Burns, S., Wessner, L., Krishnamurthy, N., Zimmerly, E., Swan, M. K., Krings, S., Muirhead, H., Chirgwin, J., and Davies, C. (2004) The crystal structure of mouse phosphoglucose isomerase at 1.6 Å resolution and its complex with

glucose 6-phosphate reveals the catalytic mechanism of sugar ring opening, *J. Mol. Biol. 342*, 847−850.
15. Arsenieva, D., and Jeffery, C. (2002) Conformational changes in phosphoglucose isomerase induced by ligand binding, *J. Mol. Biol. 323*, 77−84.
16. Davies, C., and Muirhead, H. (2003) The crystal structure of native phosphoglucose isomerase from rabbit: conformational changes associated with catalytic function, *Acta Crystallogr. D59*, 453−465.
17. Volkl, P., Huber, R., Drobner, E., Rachel, R., S., B., Trincone, A., and Stetter, K. O. (1993) *Pyrobaculum aerophilum* sp. nov., a novel nitrate-reducing hyperthermophilic archaeum, *Appl. Environ. Microbiol. 59*, 2918−2926.
18. Cleasby, A., Wonacott, A., Skarzynski, T., Hubbard, R. E., Davies, G. J., Proudfoot, A. E., Bernard, A. R., Payton, M. A., and Wells, T. N. (1996) The X-ray crystal structure of phosphomannose isomerase from *Candida albicans* at 1.7 Å resolution, *Nat. Struct. Biol. 3*, 470−479.
19. Gracy, R. W., and Noltmann, E. A. (1968) Studies on phosphomannose isomerase. III. A mechanism for catalysis and for the role of zinc in the enzymatic and the nonenzymatic isomerization, *J. Biol. Chem. 243*, 5410−5419.
20. Rose, I. A., O'Connell, E. L., and Schray, K. J. (1973) Mannose 6-phosphate: anomeric form used by phosphomannose isomerase and its 1-epimerization by phosphoglucose isomerase, *J. Biol. Chem. 248*, 2232−2234.
21. Roux, C., Lee, J. H., Jeffery, C. J., and Salmon, L. (2004) Inhibition of type I and type II phosphomannose isomerases by the reaction intermediate analogue 5-phospho-D-arabinonohydroxamic acid supports a catalytic role for the metal cofactor, *Biochemistry 43*, 2926−2934.
22. Lee, J. H., Chang, K. Z., Patel, V., and Jeffery, C. J. (2001) Crystal structure of rabbit phosphoglucose isomerase complexed with its substrate D-fructose 6-phosphate, *Biochemistry 40*, 7799−7805.
23. Chirgwin, J. M., and Noltmann, E. A. (1975) The enediolate analogue 5-phosphoarabinonate as a mechanistic probe for phosphoglucose isomerase, *J. Biol. Chem. 250*, 7272−7276.
24. Swenson, C. A., and Barker, R. (1971) Proportion of keto and aldehyde forms in solutions of sugars and sugar phosphates, *Biochemistry 10*, 3151−3154.
25. DeLano, W. L. (2002) *PYMOL*, DeLano Scientific, San Carlos, CA.

BI048608Y